Theor Chem Acc (2011) 128:411–418
DOI 10.1007/s00214-010-0828-1

REGULAR ARTICLE

Electron delocalization and bond formation under the ELF framework

J. Contreras-García · J. M. Recio

Received: 8 July 2010 / Accepted: 14 September 2010 / Published online: 27 October 2010

Abstract A first approach to the relationship between the electron localization function (ELF) and electronic delocalization upon bond formation is provided. We show from first principles the ability of ELF at the bond critical points to act as an index of the electron reorganization involved in chemical bonding. Simultaneously, this index, that we shall call ELF delocalization index (EDI), constitutes a good measure of electron delocalization. We will show how the core of ELF is proportional to the Wiberg index under the valence bond approach. This relationship will be exploited for some representative examples where EDI is able to identify the stages of bond formation. Furthermore, a maximum in EDI along this process has been found to correlate with the molecular equilibrium configuration, allowing for a formulation of a "maximal localization principle" for the stable structure of covalent compounds in terms of ELF.

Keywords Chemical bonding · Electron localization function · Electron delocalization · Bond formation

1 Introduction

In spite of the numerous analyses on molecular structural changes carried out by means of the combination of electron localization function (ELF) studies and catastrophe theory [1], we are still far from a complete conceptual understanding of the interplay between the triad energy-chemical bonding-wavefunction. This is translated within the ELF framework in not much work being devoted to establishing a thorough link between the outcome of quantum chemical calculations, in the shape of wavefunctions and densities, and the ELF bonding pattern [2]. For this purpose, it is necessary to forget the complicated shape of common wavefunctions and to collect in a simple manner the main consequences that bond formation has in Hilbert space so that we can relate them to the topological changes suffered by ELF. Due to the ability of the valence bond (VB) approach to correctly account for bond dissociation in terms of orbital interference, we will follow this VB route in order to get deeper insight into the effects of the Pauli principle on the topology of ELF. VB theory provides the fundamentals for the comprehension of chemical bonds in terms of quantum interference between clouds and the exchange interaction, correctly accounting for the dissociation of homonuclear diatomic molecules for which the molecular orbital approach spectacularly fails.

After giving in Sect. 2 some background on ELF and its ability to account for electron localization, the correlation between bond formation and ELF will be analyzed in Sect. 3. We will formulate the electron localization function within the valence bond approximation following a similar procedure to that established by Savin in terms of the excess of kinetic energy density brought about by the Pauli principle. This VB formulation will highlight the relevance of the ELF value at the *bip* for (1) providing a measure of electron delocalization and (2) comprehending bond formation. With this information, we will construct an index that we shall call EDI (*ELF Delocalization Index*). The first point will be developed in Sect. 4, where the core of ELF, $\chi(\mathbf{r})$, will be related to the excess of kinetic energy

Published as part of the special issue celebrating theoretical and computational chemistry in Spain.

J. Contreras-García (✉) · J. M. Recio
MALTA-Consolider Team and Departamento de Química Física y Analítica, Universidad de Oviedo, 33007 Oviedo, Spain
e-mail: julia@carbono.quimica.uniovi.es; julia.contreras@duke.edu

brought about by orbital orthogonalization. The ability of EDI to characterize the process of bond formation will be exploited then in some representative examples in Sect. 5, where the conclusion derived from the VB analysis will be shown to apply for MO calculations. Indeed, it will be shown how the value of EDI is able to identify the stable conformation. We will end up with a summary of the main conclusions derived from this approach.

2 Theoretical background: ELF and electron localization

The electron localization function was originally designed by Becke and Edgecombe to identify "localized electronic groups in atomic and molecular systems" [3]. As formulated by Savin et al. [4], it relies, through its kernel, to the laplacian of the conditional same spin pair probability scaled by the homogeneous electron gas kinetic energy:

$$\chi(\mathbf{r}) = \frac{\Delta t(\mathbf{r})}{t^0(\mathbf{r})}, \tag{1}$$

in which $\Delta t(\mathbf{r})$ can be understood [4–6] as the difference of the actual definite positive kinetic energy $t(\mathbf{r})$ and the von Weizsäcker kinetic energy density [7], that solely depends on the density, ρ:

$$\Delta t = t(\mathbf{r}) - \frac{1}{4}\frac{(\rho(\mathbf{r}))^2}{\rho(\mathbf{r})} \tag{2}$$

Division by $t^0(\mathbf{r})$ establishes a reference with the kinetic energy density of the homogeneous electron gas:

$$t^0(\mathbf{r}) = \frac{3}{5}(6\pi^2)^{2/3}\rho^{5/3}(\mathbf{r}) \tag{3}$$

For convenience reasons, the function $\chi(\mathbf{r})$ is re-scaled according to $ELF = (1+\chi^2)^{-1}$, so that it runs from 0 to 1 and high values of the function correspond to regions of high localization.

Several interpretations of ELF have been proposed along the years. For our coming discussion, it is interesting to note that previous interpretations in terms of orbitals were advanced by Burdett [8] and more recently by Nalewajski et al. [9] who considered the non-additive inter orbital Fisher information. Another route is to explicitly consider pair functions [10], an approach that has been independently developed by Kohout et al. [11, 12] and by Silvi [13, 14].

The topological partition of the ELF gradient field [15, 16] yields basins of attractors that can be thought of as corresponding to atomic cores, bonds and lone pairs. The valence basins V(A, ...) encompassing a given atomic core basin C(A) form the valence shell of atom A, in agreement with the Lewis's picture, and they may belong to several atomic shells. Moreover, it has been recently shown that the electrostatic repulsions between these basins provide a justification of the valence shell electron pair repulsion (VSEPR) rules [17]. The properties of the gradient dynamical system are complemented with the interpretation derived from the concept of *f*-domain [18], which enables to recover chemical units in the system, as well as to characterize the basins according to common chemical knowledge. According to the value of ELF at the first-order saddle points where the *f* domains change, also known as *bips* (bond interaction points) [19] or (3, −1) critical points [20], a bifurcation tree can be constructed that reveals the basin hierarchy at a glance [2, 18].

Throughout the text, several computational codes have been used for the analysis of ELF profiles and topology. The equations derived in Sect. 3 have been implemented in `gnuplot`. The analysis of molecular topologies at the Hartree-Fock level has been carried out with the `TOPMOD` package [21]. A special version of the code has been developed for the 1D plots (e.g. Fig. 5). Applications to crystalline solids have been analyzed thanks to a code developed by the authors [22] that enables local and global topological analysis from crystalline wavefunctions.

3 Characterization of bond formation

In order to achieve a good description of the process of bond formation under the ELF approach, it is necessary to invoke a supermolecular wavefunction able to qualitatively reproduce the interactions brought about by the pairing of electrons.

3.1 ELF within the valence bond approximation

In this section, we will resort to the valence bond wavefunction in order to further analyze how the changes in the control parameters (nuclei positions) influence the wavefunction and induce electron pairing in real space as pictured by ELF.

We first set down the usual elementary treatments of the two electron bond, such as in H_2. We use atomic orbitals ψ_A (atom A) and ψ_B (atom B) as the building blocks, with overlap $S = \int \psi_A \psi_B d\tau$.

The Heitler-London [valence bond (VB)] wavefunction that results is given by orbital orthogonalization according to [23]:

$$\phi(1,2)\frac{1}{\sqrt{1+S^2}}(\psi_A(1)\psi_B(2) + \psi_A(2)\psi_B(1)) \tag{4}$$

So that the density (ρ) and the positively defined kinetic energy density (t) can be obtained, respectively, by:

$$\rho(\mathbf{r}) = \int |\phi|^2 \mathrm{d}\mathbf{r}_2$$
$$= \frac{1}{1+S^2}\left(\psi_A^2(\mathbf{r}) + \psi_B^2(\mathbf{r}) + 2S\psi_A(\mathbf{r})\psi_B(\mathbf{r})\right) \quad (5)$$
$$= \frac{1}{1+S^2}\left(\rho_A(\mathbf{r}) + \rho_B(\mathbf{r}) + 2S\psi_A(\mathbf{r})\psi_B(\mathbf{r})\right) \quad (6)$$

and

$$t(\mathbf{r}) = \frac{1}{2}\int |\nabla\phi|^2 \mathrm{d}\mathbf{r}_2 = \frac{1}{2(1+S^2)}\left(\nabla\psi_A^2(\mathbf{r}) + \nabla\psi_B^2(\mathbf{r}) + 2S\nabla\psi_A(\mathbf{r})\nabla\psi_B(\mathbf{r})\right) \quad (7)$$
$$= \frac{1}{1+S^2}\left(t_A + t_B + S\nabla\psi_A\nabla\psi_B\right) \quad (8)$$

since $\rho_A = |\psi_A|^2$ and $t_A = \frac{1}{2}|\nabla\psi_A|^2$. The difference between $t(\mathbf{r})$ before and after the antisymmetrization provides a good approximation to the changes due to the fermionic nature of electrons. It can be understood as the interference term that results from subtracting the classical contribution to Eqs. 6 and 8:

$$\Delta\rho(\mathbf{r}) = \frac{-S^2}{1+S^2}\left(\psi_A^2(\mathbf{r}) + \psi_B^2(\mathbf{r})\right) + \frac{2S}{1+S^2}\psi_A(\mathbf{r})\psi_B(\mathbf{r}), \quad (9)$$

$$\Delta t(\mathbf{r}) = t^I(\mathbf{r}) + t^{II}(\mathbf{r}) \quad (10)$$
$$= \frac{-S^2}{2(1+S^2)}\left(\nabla\psi_A^2(\mathbf{r}) + \nabla\psi_B^2(\mathbf{r})\right) + \frac{S}{1+S^2}\nabla\psi_A(\mathbf{r})\nabla\psi_B(\mathbf{r}) \quad (11)$$

The mono- and bicentric contributions ($t^I(\mathbf{r})$ and $t^{II}(\mathbf{r})$) to the kinetic energy density have been highlighted for ulterior discussion. From Eq. 11, we can proceed to define and analyze ELF under the VB approach, $ELF^{VB} = \left(1 + (\chi^{VB})^2\right)^{-1}$, with:

$$\chi^{VB} = \frac{\Delta t(\mathbf{r})}{t^0(\mathbf{r})} \quad (12)$$

where t^0 is given by Eq. 3. The clear relationship between χ^{VB} and the interacting orbitals by means of Eqs. 6 and 11 will proof to be very useful in the coming sections for understanding delocalization and bond formation.

3.2 The ELF delocalization index (EDI)

The results of the interference are easily analyzed at the bond middle point, $R/2$, although they are apparent along the whole bonding region. For a homonuclear diatomic molecule, $\Delta\rho$ and Δt at this point are given, respectively, by:

$$\Delta\rho\left(\frac{R}{2}\right) = \frac{2S(1-S)}{1+S^2}\rho_A\left(\frac{R}{2}\right) > 0 \quad (13)$$

$$\Delta t\left(\frac{R}{2}\right) = \frac{-2S(1+S)}{1+S^2}t_A\left(\frac{R}{2}\right) < 0 \quad (14)$$

where we have made use of the contragradience relationship $\nabla\psi_A(R/2) = -\nabla\psi_B(R/2)$. These relationships highlight the main characteristics of the exchange contribution in the bonding region: density increases and electrons become slower. The net effect on the ELF value at the bond point is a rise that identifies the interference taking place. Although the nature of the critical point might change (a maximum will appear if the covalent bond is finally formed), the value of ELF at this "bond point" enables the characterization of the process of bond formation. We shall call this value EDI from now onwards after "ELF delocalization index".

In order to visualize the evolution of EDI and delocalization upon bond formation, it is possible to resort to ELF^{VB} defined in Eq. 12. However, this information cannot be exploited directly due to the impossibility of ELF to reflect bonding in the two electron case. As already observed for the MO approach, the fact that ELF is based on same spin probabilities gives a value of 1 in the whole space for the 2 electron case, i.e. for the 2 orbital- 2 electrons for which the above VB approach is developed. In spite of this conceptual difficulty, it is possible to understand the process of bond formation from the analysis of the monocentric and bicentric terms in Eq. 11. The aforementioned contragradience of orbitals led Goddard and Wilson [24] to advance that the bicentric contribution to the kinetic energy is the main responsible for the localization of electrons in the bonding region. However, a closer look at the definition of this contribution reveals that this is not the case. As shown above, the effect of electron pairing in the bonding region is a decrease in their electronic kinetic energy, a fact that can only be accounted for by $t^I(\mathbf{r})$. Analysis of $t^{II}(\mathbf{r})$ along the internuclear line would clearly unveil a straight line for a given R. This fact is easily understood in terms of the H_2 molecule with a STO basis set (exponent $\zeta = 1$):

$$t^{II}(\mathbf{r}) = \frac{S}{1+S^2}\nabla\psi_A(\mathbf{r})\nabla\psi_B(\mathbf{r}) = \frac{S}{1+S^2}e^{-R} \quad (15)$$

The influence of both terms upon bond formation can be actually visualized if ELF is constructed from each of the contributions:

$$\chi = \sum_i \chi^i = \sum_i \frac{t^i(\mathbf{r})}{t^0(\mathbf{r})}, \quad (16)$$

$$ELF\left[t^i\right] = \frac{1}{1+(\chi^i)^2} \quad (17)$$

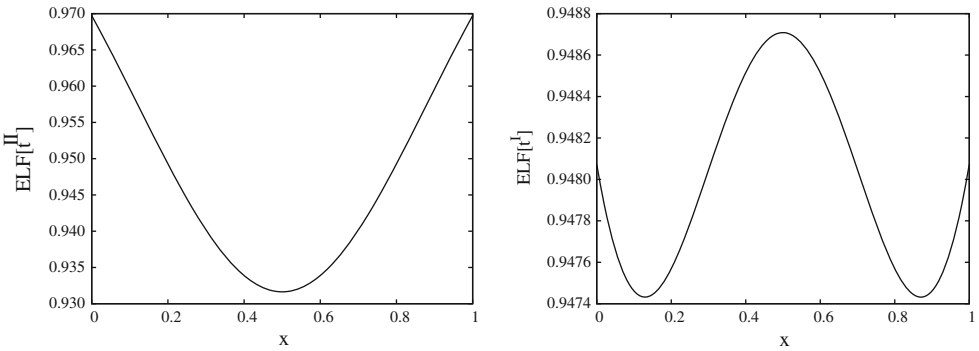

Fig. 1 ELF from the monocentric (*right*) and bicentric (*left*) contributions to the kinetic energy density upon the interference of two STO orbitals with exponent $\zeta = 1$ along the bonding direction of two H atoms at $R = 1.0$ bohr (atoms are placed at $x = 0$ and $x = 1$)

where i stands for the mono- and bicentric contributions (Eqs. 14, 15). Although the resulting $ELF[t^i]$ are obviously non-additive, much information can be gained from their analysis. Since t^{II} is constant, $ELF[t^{II}]$ (Fig. 1 left) only gathers information from the electron density: it reflects the atomic positions. Local information about the chemical bond arises from the monocentric contribution, t^I, so that $\mathrm{ELF}[t^I]$ (Fig. 1 right) reflects the net localization of electrons in the interatomic region. This result is in agreement with the relevance given by Ruedenberg [25] to the monocentric interference population in bonding stabilization.

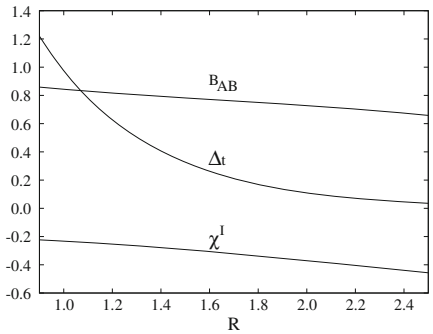

Fig. 2 Correlation between the Wiberg index and χ^I under the VB approximation for the H_2 molecule described with a minimal STO basis (exponent $\zeta = 1$). R is the interatomic distance in a.u

4 Characterization of bond order

The evolution of bond orders provides an intuitive visualization of the progress of electronic reorganization along a reaction path. Hence, it is not surprising to find that electron distribution indexes are equivalent to delocalization indexes [26, 27]. In agreement with recent analyses that highlight the ability of the Hartree-Fock approach to characterize the densities involved in many processes of bond formation [28, 29], ELF can be understood as a one-electron measure of electron fluctuation. The relationship between the value of ELF along the interacting line and inter-basin delocalization is easily inferred from Eqs. 13 and 14. As fragments approach one another, electrons flow from the atom/molecule to the interfragment region and ELF rises at those places where it was earlier negligible, such as the first-order saddle points or bond interaction points (*bips*). Indeed, the greater the *bip* value, the closer the relationship between the basins involved [30].

In order to analyze the ability of ELF as a delocalization index, let's go back to our test-bed case, the perfect homonuclear H_2 molecule under the VB approach. Resorting to the Wiberg index [31], which is probably the widest spread measure of electron delocalization, we have under the same methodology [32]:

$$B_{AB}^{VB} = 4\left(\frac{S(1+S)}{1+S^2}\right)^2 \tag{18}$$

The overlap term is exactly the same as the one for the Pauli kinetic energy term in Eq. 14 at the (3, –1) critical point. This finding further confirms the relevancy of the "bond point" at which EDI is analyzed in understanding bond formation. Moreover, we have then arrived at a simple and clear relationship between the variations induced in the kinetic energy density in the bond region and the bond order of molecules. Results for these two quantities in our test-bed H_2 molecule are shown in Fig. 2. Two regions clearly arise from the analysis of $\Delta t(\mathbf{r})$. For about $R > 2$, where density changes are small compared to the kinetic energy ones, the behavior of the Wiberg index is completely determined by the variation in the kinetic energy induced by the interference [33]. At smaller distances, B_{AB} and Δt do not follow the same behavior. However, the homogeneous electron gas rescaling is able to get rid of the density dependency so that the parallelism between B_{AB} and χ^I is preserved. It is interesting to note that this analysis not only enables to understand the need to rescale the Pauli kinetic energy in order to obtain a good picture of bonding, but most importantly, it is able to show

the relationship between the EDI value and delocalization measures. In fact, the relationship between ELF in the bonding region and electron delocalization has been stealthily present in the literature.

Firstly, the interpretation of ELF by Putz [34] in terms of the relative error in electronic position and momentum highlights the relevance of ELF lower values (in those regions, the uncertainty in the spatial localization of the electrons is very low). This delocalization interpretation is also associated with the proposal by Savin to link perfect ELF basins with perfectly localized orbitals [35, 36]. In this hypothetical case, the overlap fulfills $S_{ij}(\Omega) = \delta_{ij}$, so that the overlap at the border of the perfectly localized orbital is zero and so is the ELF, since $t(\mathbf{r}) = \nabla\psi(\mathbf{r}) = \infty$. In the opposite case, that of metals, we also have the index proposed by Silvi and Gatti [37], where the EDI value is used to measure metallicity. Kohout [38] also proposed an alternative measure of localization (ELI) that coincides with ELF at the Hartree-Fock level. ELI, which is defined without the reference to the uniform electron gas, integrates the electron pair density over regions of fixed spin charge. Thus, it highlights more clearly the variation between 0 and 1 in ELF/ELI with an augmentation of the correlation between same spin electrons. Furthermore, the wide-spread use of bifurcation diagrams [15, 18, 19] to understand the relationship between chemical entities is based on this very same principle. As the ELF at the *bip* point is larger, the chemical entities separated by it are more interrelated, i.e. there is a greater delocalization between them.

This result also throws light into the meaning of the integrations within the basins delimited by zero flux ELF surfaces. The relationship of ELF with the charge-independent curvature of the Fermi hole [10] indicates that ELF separatrices are connected with the existence of minimum inter-basin delocalization. Therefore, ELF would divide the space in regions analogous to the *loges* of Daudel [39]. Indeed, the fact that the charges provided by the integration of the ELF basins are so close to the chemically expected values clearly indicates that these basins enclose the chemical meaning of electronic pairing.

All in all, these ideas point in the direction of taking ELF as a tool that divides space into regions of maximal localization, whose separation from one another is reflected in the EDI value. A deep analysis of the localization pattern of a chemical system should not only include the value of ELF at the maxima, but also the EDI values, in order to provide insight into the variance of the associated populations.

5 Application to molecules and solids

5.1 Valence bond in the H_2 molecule

In order to check the ability of χ^I to reproduce the process of bond formation, let's take again the ground state of the H_2 molecule, where most of the binding energy stems from the exchange-overlap term. It is well set that the VB approach provides a good qualitative description of the ground state interaction, and, most importantly, it gives rise to a good description of the H_2 dissociation. As expected, electrons are only localized at the nuclei for long H–H distances (Fig. 3 left), whereas a bonding region appears as the atoms come closer together (Fig. 3 right). At large distances, where virtually no overlap exists between orbitals, the main contribution to energy is due to the correlation of electrons, not accounted for in the HF approximation, and not reflected in the ELF picture (Fig. 3 left). As orbitals come closer together, their overlap is not negligible anymore and exchange interaction arises [40]. The new overlap between orbitals gives rise to a non-negligible probability of electrons being in both fragments. According to the Pauli principle, this overlap requires the antisymmetrization of the corresponding orbitals [41] and gives rise to the formation of the bond (see Fig. 3 right).

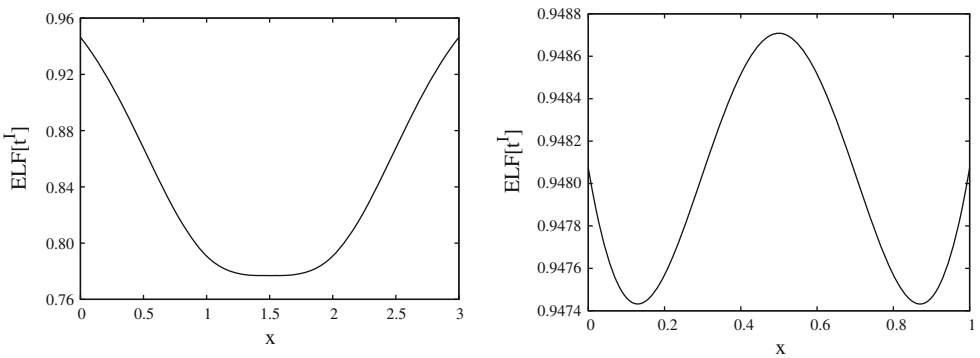

Fig. 3 Valence bond ELF profiles in H_2 for $R = 3.0$ a.u. (*left*) and $R = 1.0$ a.u. (*right*). We have assumed the exponent ζ to be 1

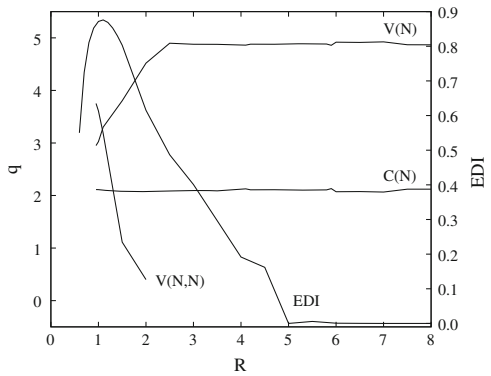

Fig. 4 Evolution of basin charges (q) and EDI upon bond formation in N_2. The equilibrium geometry is found around $R = 1$ bohr. Distances and charges in atomic units

5.2 Hartree-Fock in the N_2 molecule

It has been argued that the independent electron approximation (HF) provides in many cases [14, 29] a good description of chemical bonding, and hence, the pair density descriptors can be approximated by charge-dependent indexes. This picture would be in agreement with the association of bond charges, N_b, with bonding indexes [15] $B_{AB} \simeq 0.5\ N_b$, as well as with the observation of bond order conservation along exchange reactions [42]. It becomes thus interesting to check the applicability of EDI to other calculation methods, so we will study the process of bond formation in N_2 under the MO-HF approach. It exemplifies the evolution of EDI upon dissociation of a covalent multiple bond within HF (Fig. 4) and can be compared with previous studies of bond formation [43, 44]. The bonding changes that have been found, as well as their regimes, are in agreement with recent Fermi Hole based (SEDI and DAHF) results [29].

Figure 5 shows that at $R = 5.0$, we are still in an atomic-like regime: the EDI value is negligible and there is no bond basin (see Fig. 4). At $R = 4.5$ bohr only polarization takes place, the EDI value is rising but a disynaptic basin is still lacking. At $R = 2.0$ bohr, the V(N,N) appears (Fig. 4). As the molecule is further compressed, bond basin charge continuously grows. At $R \simeq 1.0$, the N–N disynaptic basin is completely formed and separated from the lone pairs. As expected from the process, the EDI value increases along the bond formation process, identifying the increasing N–N bond order. Furthermore, a very interesting feature appears under the HF approach. The EDI reaches its maximum at the equilibrium conformation and then decreases again. This is an extremely appealing test to which many bond orders fail. Density-only-based

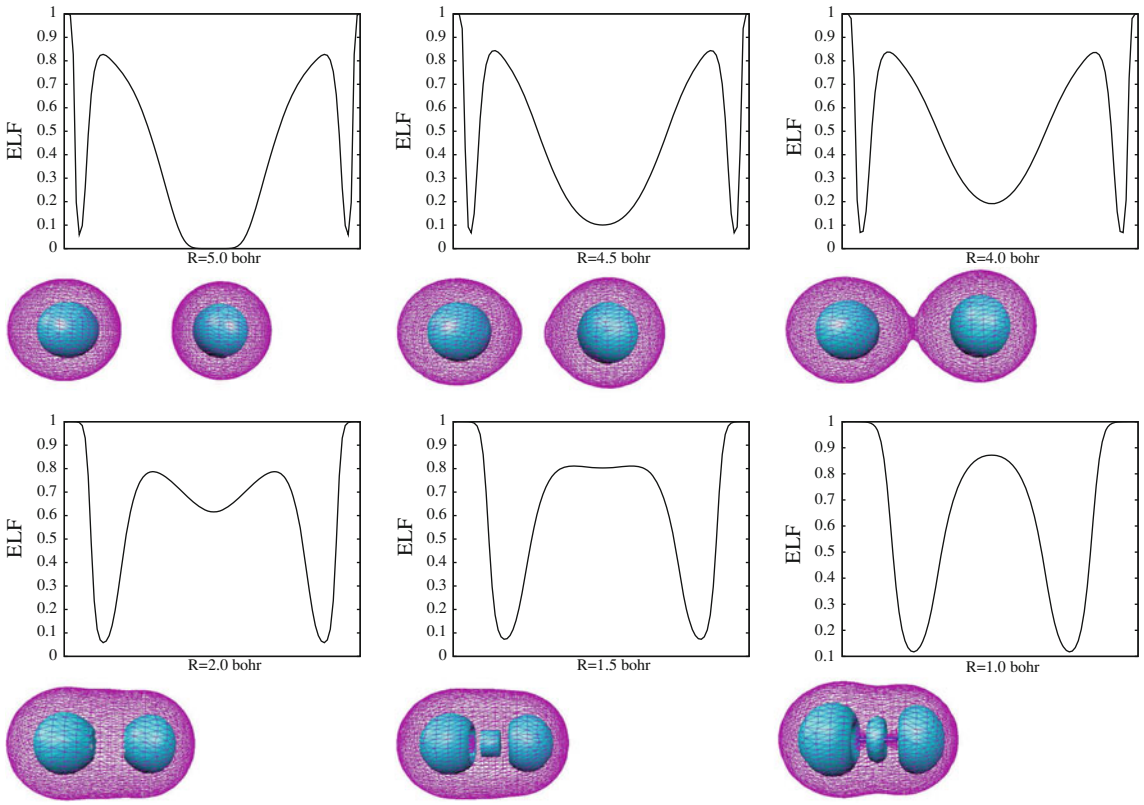

Fig. 5 Evolution of ELF profiles (*top*) and isosurfaces (*bottom*) for different bonding regimes in N_2. *Blue* and *purple* isosurfaces highlight core and valence, respectively

approaches continuously increase as the molecule is compressed, independently of being at the repulsive wall. As an example, basin charges are provided in Fig. 4. However, the inclusion of kinetic energy densities provides more insight into the formation of the bond, identifying the equilibrium geometry.

5.3 Solid CO_2

One of the most appealing applications of EDI as a delocalization measure is the study of interactions in solid state. Delocalization indexes have been providential in the study of multicenter interactions within molecules [15, 45], but their calculation in crystalline phases is limited due to the difficult access to high-order density matrixes in solid calculations. Indeed, the recent availability of high-pressure techniques has enabled the identification of many bond formation processes, whose study is crucial from a theoretical point of view. The application of the principles we have hereby developed encloses a great potentiality in this area.

The analysis of CO_2 polymerization enables to illustrate the ability of EDI to track the process of bond formation in solids. Figure 6 shows the evolution of the ELF profile as CO_2 proceeds towards 6-fold polymerization, highlighting the increase in EDI and thus the relevance of exchange interaction upon bond formation. At large cell volumes (Fig. 6 left), the molecular phase is the stable polymorph, i.e. the multiple C=O bond of different fragments is favored over an extended single bond network. Hence, molecular units that respect the *in vacuo* geometries, separated by great distances between them, are observed. Indeed, the inspection of the intramolecular bond in Fig. 6 (left,bottom) reveals a ring shape for the bond attractors, a fingerprint of double bonds. The intermolecular forces that retain the CO_2 molecules together in this range are long range, and virtually, no overlap between the orbital fragments occurs. As the volume is further compressed, the approach of surrounding molecules induces chemical changes in the molecular structure (Fig. 6 center). The EDI value in the intermolecular region between intermolecular valencies rises (see Fig. 6 center, top), highlighting the drastic contribution of electronic exchange to polymerization [30]. This intermolecular interaction has a net effect on the molecule itself. A weakening of the intramolecular C–O bond takes place, which is observed in the loss of its annular shape and in the decrease of its electron population. As pressure is induced, the density reorganization of the lone pairs gives rise to new lone pair maxima oriented towards the approaching molecule that represents the "secondary interactions" (see attractors in Fig. 6 center, bottom). The emerging basin can be considered as a prelude to a future bond, giving rise to a 2 + 4 carbon coordination. This fact would explain the incipient stabilization of a 6-fold coordinated carbon (stishovite-like) at high pressure. At higher compression (Fig. 6 right), a new covalent bond in completely formed with the 4 s neighbors giving rise to an extended single bond framework.

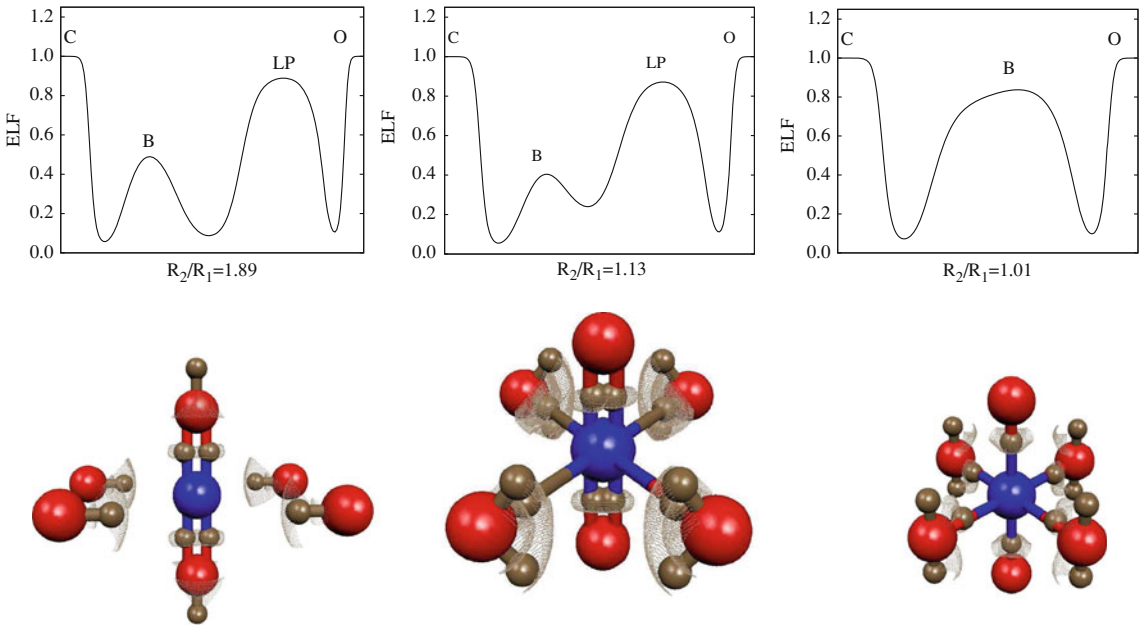

Fig. 6 Evolution upon compression of ELF profiles (*top*) and isosurfaces (*bottom*) for different bonding regimes along CO_2 polymerization. *Top* ELF profiles and their chemical meaning: C for carbon, O for oxygen, B for bond and LP for lone pair. *Bottom* first and second neighboring oxygens (*red*) for one carbon atom (*blue*) are shown. Valence atttractors and isosurfaces in brown. R_1 and R_2 refer to the distance to the first and second neighbors, respectively

6 Conclusions

We have introduced a formulation of the electron localization function within the valence bond approach, which allows to understand the qualitative changes that this function suffers upon bond formation. Moreover, the analysis of these changes enables to relate the EDI value (ELF value at the bond point) with electron delocalization, hence introducing an easy and visual monoelectronic index for pair fluctuation. This finding is especially relevant for solid state calculations, whereby pair density-related fluctuation indexes are not easily available. Finally, the relationship between delocalization and electron reorganization along the bond formation path has been exploited in some representative examples, showing the inherent correlation between the stability and the electron localization within a molecule. It has been found that the equilibrium geometry is driven toward a maximum in the EDI, allowing for a formulation of a "maximal localization principle" for the stability of covalent compounds.

Acknowledgments Financial support from the Spanish MEC and FEDER program under project CTQ2009-14596-C02-02 is gratefully acknowledged. JCG wants to thank the Spanish MEC for a FPU postgraduate grant. Most of the calculations have been performed under the MALTA-Computer facility and at the Universidad de Oviedo (CSD2007-00045).

References

1. Krokidis X, Noury S, Silvi B (1997) J Phys Chem A 101:7277
2. Savin A, Silvi B, Colonna F (1996) Can J Chem 74:1088
3. Becke AD, Edgecombe KE (1990) J Chem Phys 92:5397
4. Savin A, Jepsen O, Flad J, Andersen L, Preuss H (1992) Angew Chem Int Ed Engl 31:187
5. Savin A, Nesper R, Wengert S, Fässler TF (1997) Angew Chem Int Ed Engl 36:1809
6. Savin A, Becke AD, Flad J, Nesper R, Preuss H, von Schnering HG (1991) Angew Chem Int Ed Engl 30:409
7. von Weizsäcker CF (1935) Z Phys 96:431
8. Burdett JK, McCormick TA (1998) J Phys Chem A 102:6366
9. Nalewajski RF (2005) J Phys Chem A 109:10038
10. Dobson JF (1991) J Chem Phys 94:4328
11. Kohout M, Pernal K, Wagner FR, Grin Y (2004) Theor Chem Acc 112:453
12. Kohout M, Pernal K, Wagner FR, Grin Y (2005) Theor Chem Acc 113:287
13. Silvi B (2003) J Phys Chem A 107:3081
14. Matito E, Silvi B, Durán M, Solá M (2006) J Chem Phys 125:024301
15. Silvi B, Savin A (1994) Nature 371:683
16. Häussermann U, Wengert S, Nesper R (1994) Angew Chem Int Ed Engl 33:2069
17. Martín Pendás A, Francisco E, Blanco MA (2008) Chem Phys Lett 454:396
18. Calatayud M, Andrés J, Beltrán A, Silvi B (2001) Theor Chem Acc 105:299
19. Kohout M, Wagner FR, Grin Y (2002) Theor Chem Acc 108:150
20. Bader RFW (1990) Atoms in molecules: a quantum theory. Oxford University Press, Oxford
21. Zoury S, Krokidis X, Fuster F, Silvi B (1999) Comput Chem 23:597. See also: http://www.jussieu.fr/silvi
22. Contreras-García J, Martín Pendás A, Silvi B, Recio JM (2009) J Chem Theory Comp 5:164
23. Heitler W, London F (1927) Z Phys 44:455
24. Goddard WA, Wilson CW Jr (1972) Theor Chim Acta (berl.) 26:211
25. Ruedenberg K (1962) Rev Mod Phys 34:326
26. Ponec R, Yuzhakov G, Cooper DL (2003) J Phys Chem A 107:2100
27. Fradera X, Austen MA, Bader RFW (1999) J Phys Chem A 103:304
28. Mayer I (2007) Faraday Discuss 135:131
29. Cooper DL, Ponec R (2008) Phys Chem Chem Phys 10:1319
30. Contreras-García J, Martín Pendás A, Silvi B, Recio JM (2009) J Phys Chem B 113, 1068
31. Wiberg KB (1968) Tetrahedron 24:1083
32. de Giambiagi MS, Giambiagi M, Jorge FE (1985) Theor Chim Acta 68:337
33. Feinberg MJ, Ruedenberg K (1970) J Chem Phys 54:1495
34. Putz MV (2005) Int J Quantum Chem 105:1
35. Savin A (2005) J Chem Sci 117:473
36. Savin A (2005) J Molec Struct 727:127
37. Silvi B, Gatti C (2000) J Phys Chem A 104:947
38. Kohout M (2004) Int J Quantum Chem 97:651
39. Daudel R, Brion H, Odiot S (1955) J Chem Phys 23:2080
40. Kitaura K, Morokuma K (1976) Int J Quant Chem 10:325
41. Bickelhaupt FM, Baerends EJ (2000) Rev Comput Chem 15:1
42. Johnson HS (1960) Adv Chem Phys 3:131
43. Ponec R, Cooper DL (2007) Faraday Discuss 135:31
44. Ponec R, Yuzhakov G, Cooper DL (2003) J Phys Chem A 107:2100
45. Fässler TF, Savin A (1997) Chem Unserer Zeit 31: 110